



# Desymmetrization of meso diols using enantiopure zinc (II) dimers: Synthesis and chiroptical properties

Eswaran Chinnaraja<sup>1,2</sup> | Rajendran Arunachalam<sup>1,2</sup> | Jayanta Samanta<sup>2,3</sup> |  
Ramalingam Natarajan<sup>2,3</sup> | Palani S. Subramanian<sup>1,2</sup>

<sup>1</sup>Inorganic Materials and Catalysis Division, CSIR-Central Salt and Marine Chemicals Research Institute (CSIR-CSMCRI), Bhavnagar 364 021 Gujarat, India

<sup>2</sup>Academy of Scientific and Innovative research (AcSIR), Ghaziabad 201 002, India

<sup>3</sup>Organic & Medicinal Chemistry Division, CSIR-Indian Institute of Chemical Biology, Kolkata, India

## Correspondence

Palani S. Subramanian, Inorganic Materials and Catalysis Division, CSIR-Central Salt and Marine Chemicals Research Institute (CSIR-CSMCRI), Bhavnagar- 364 021, Gujarat, India. Email: siva140@yahoo.co.in

## Funding information

DST-SERB New Delhi, Grant/Award Numbers: SB/S1/IC-26/2013 and SR/S1/IC-23/2011

The one-pot metal templated synthesis of enantiopure binuclear Zn (II) complexes  $Zn_2L^1-Zn_2L^4$  were obtained by treating (1*R*,2*R*)-diphenylethylenediamine or (1*S*,2*S*)-diphenylethylenediamine with 2-hydroxy-5-methyl-1,3-benzenedicarboxaldehyde or 4-*tert*-butyl-2,6-diformylphenol and zinc acetate. The chiroptical properties of the complexes were studied by using circular dichroism spectroscopy. These  $\Delta\Delta$  and  $\Lambda\Lambda$  complexes were used as enantioselective catalysts for desymmetrization of meso diol to achieve monobenzoylated product with 96% yield and 88% *ee*.

## KEYWORDS

binuclear zinc complexes, chiroptical properties, desymmetrization, macrocycle, one-pot synthesis

## 1 | INTRODUCTION

Meso diols of cyclopentane, cyclohexane, cyclooctane and 1,2-diphenylethylene, etc. are known to possess  $C_2$  symmetry. Such diols are widely used in their symmetrical and unsymmetrical forms as building blocks in various pharma and organic compounds.<sup>[1]</sup> Nadolol, the well-known  $\beta$ -blocker, contains a meso diol.<sup>[2]</sup> Conversion of an achiral or meso compound to an enantiorich chiral product by destructing the  $C_2$  symmetry is known to be one of the highly challenging steps in such a desymmetrization reaction.<sup>[3]</sup> Desymmetrized diols are generally obtained by implying biocatalysis, for example, BCL (*Burkholderia capacia lipase*) enzyme.<sup>[4]</sup> Further, the enantiorich desymmetrized products of monoesters were also achieved by adapting various organo,<sup>[5]</sup> metal

complexes,<sup>[6]</sup> phosphine<sup>[7]</sup> and phosphinite catalysts.<sup>[8]</sup> Enzymatic<sup>[9]</sup> and kinetic resolution methods<sup>[10]</sup> were also explored extensively. As desymmetrization of meso diols is considered one of the highly challenging reactions, the metal-based chiral catalysts are considered superior. Stereoselective acylation products are important components in the preparation of various precursors in pharmaceutical and organic industries, and natural product synthesis.<sup>[11]</sup> In this regard, although many catalysts are reported,<sup>[12,13]</sup> a need for the development of a new catalyst that aims to achieve high *ee* and yield depending upon the stereochemical-fit between the catalyst-substrates and the lack of recyclability, etc. is considered essential. In this regard, many homo- and heteronuclear complexes that are reported for their selectivity, copper-<sup>[14]</sup> and zinc-based homodimers<sup>[15]</sup> are found to

be efficient. Keeping this in mind, aiming to develop a new chiral catalyst with an enhanced stereoselectivity and recyclability at ambient conditions, we have recently reported similar binuclear copper complexes<sup>[16]</sup> and mononuclear zinc complexes<sup>[17]</sup> as efficient catalysts with high yield, *ee* and recyclability. In the present manuscript, we report very simple and easy-to-synthesize binuclear chiral complexes, which are efficient at catalysing such desymmetric acylation reactions. This procedure, thus by-passing the multistep synthetic complexities in the previous reports, provides a very simple and single-step synthetic approach<sup>[18]</sup> to achieve enantiopure catalysts for such desymmetric acylation.

## 2 | RESULTS AND DISCUSSION

The binuclear enantiopure complexes  $[\text{Zn}_2(\text{RRRR})\text{-L}^1(\text{OAc})_2]$  (**1**),  $[\text{Zn}_2(\text{SSSS})\text{-L}^2(\text{OAc})_2]$  (**1'**),  $[\text{Zn}_2(\text{RRRR})\text{-L}^3(\text{OAc})_2]$  (**2**) and  $[\text{Zn}_2(\text{SSSS})\text{-L}^4(\text{OAc})_2]$  (**2'**) were prepared by the one-pot metal template method by treating stepwise 2-hydroxy-5-methyl-1,3-benzenedicarboxaldehyde (4-MDFP), or 4-*tert*-butyl-2,6-diformylphenol (4-*t*BDFP) with zinc (II) acetate followed by either (*1R,2R*)-diphenylethylenediamine [(*1R,2R*)-DPEN] or (*1S,2S*)-diphenylethylenediamine [(*1S,2S*)-DPEN], as shown in Scheme 1. A minor modification in the approach of Gao

*et al.*<sup>[19]</sup> enhanced the yield to 80–82% (Scheme 1), and simplified the synthetic complexity into a single step as described in the Experimental section. The *m/z* values of ESI-MS for **1** (*m/z* = 975.66), **1'** (*m/z* = 865.99), **2** (*m/z* = 951.11) and **2'** (*m/z* = 951.44) that are observed correspond to monocations calculated as *m/z* = 975.23, 865.97, 951.26 well, respectively.

The <sup>1</sup>H-NMR spectra of the complexes showed two distinguishable singlets at  $\delta$  = 8.25, 8.05 ppm corresponding

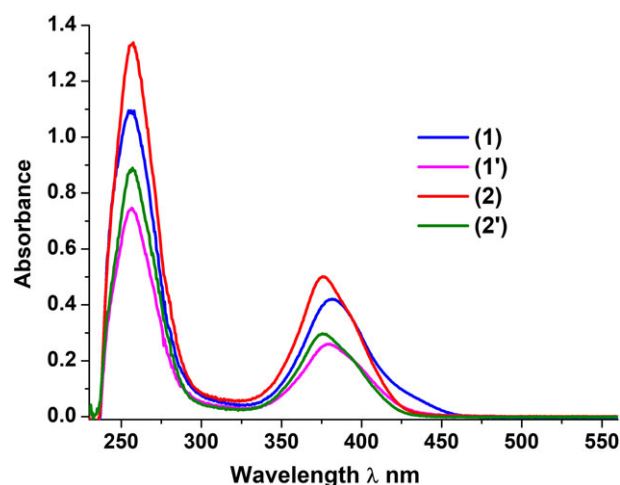
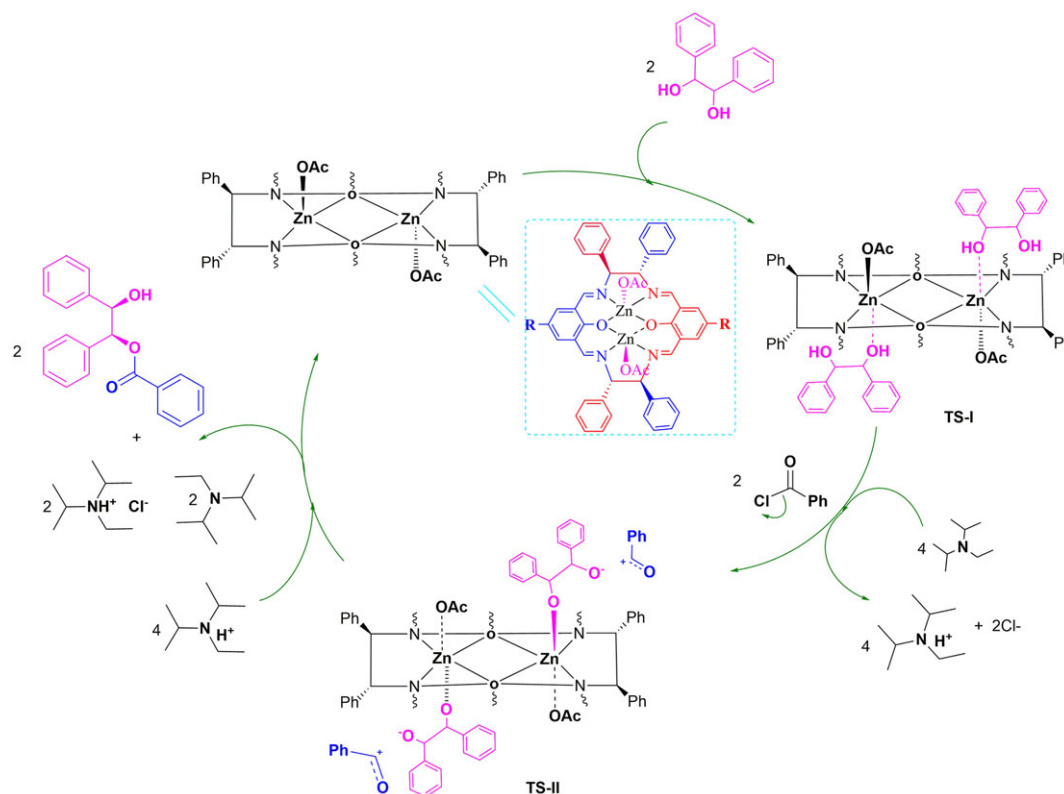
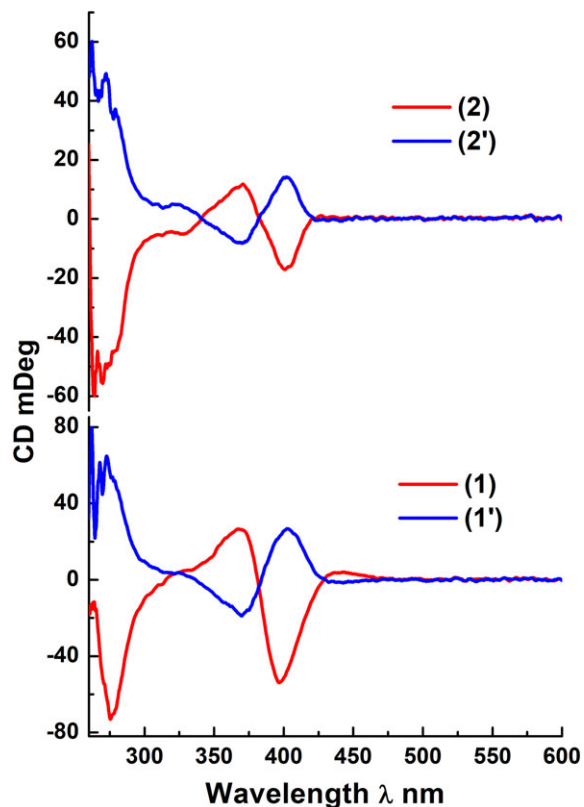


FIGURE 1 UV-Vis spectra of **1**, **1'**, **2** and **2'** in THF ( $1 \times 10^{-5}$  M)



SCHEME 1 Enantiopure Zn (II) dimers by metal template method



**FIGURE 2** Circular dichroism (CD) spectra of enantiopure dinuclear zinc complexes **1** & **1'**, **2** & **2'** ( $1 \times 10^{-4}$  M)

to the CH=N group, which fits well with the integral value of two hydrogens; and a multiplet at  $\delta = 7.3\text{--}7.40$  ppm corresponds to 24 hydrogens in the aromatic region and a singlet at  $\delta = 2.14$  ppm is attributable to the methyl group, which together confirm the formation of macrocyclic zinc (II) dimeric complex (Figures S5–S7). Electronic absorption spectra of the complexes **1**, **1'**, **2** and **2'** almost resemble each other, with two well-resolved bands at 256–257 and 375–381 nm attributed to the  $\sigma\text{-}\pi^*$ ,  $\pi\text{-}\pi^*$  transitions and LMCT transitions [phenolate oxygen to Zn (II) centre], respectively (Figure 1).

The circular dichroism (CD) spectra of **1**, **1'** and **2**, **2'** in Figure 2 reveal an opposite cotton effect at 400 nm with positive and negative signs. The equal and opposite optical behaviour obviously indicate that the complexes are in enantiopure form. The ligands **L**<sup>1</sup> and **L**<sup>3</sup> constructed with an enantiopure 1,2-diphenylethylenediamine possess *RRRR* components and produce a macrocyclic complex with  $\Lambda_M R_C = \Lambda\Lambda\text{-}[\text{Zn}_2(\text{RRRR})\text{-L}^{1,3}]$  in **1** and **2**, while the other ligands **L**<sup>2</sup> and **L**<sup>4</sup> holding the opposite enantiomer possess *SSSS* configuration and produce  $\Delta_M S_C = \Delta\Delta\text{-}[\text{Zn}_2(\text{SSSS})\text{-L}^{2,4}]$  in the complexes **1'** and **2'**. Having used enantiopure (*1R,2R*)-DPEN or (*1S,2S*)-DPEN, the enantiopurity of the complexes **1**, **1'**, **2** and **2'** is beyond doubt. All the metal centres in these complexes possess pentacoordinated geometry, and the assignment of the chiral descriptors  $\Delta$  and  $\Lambda$  is possible in principle.

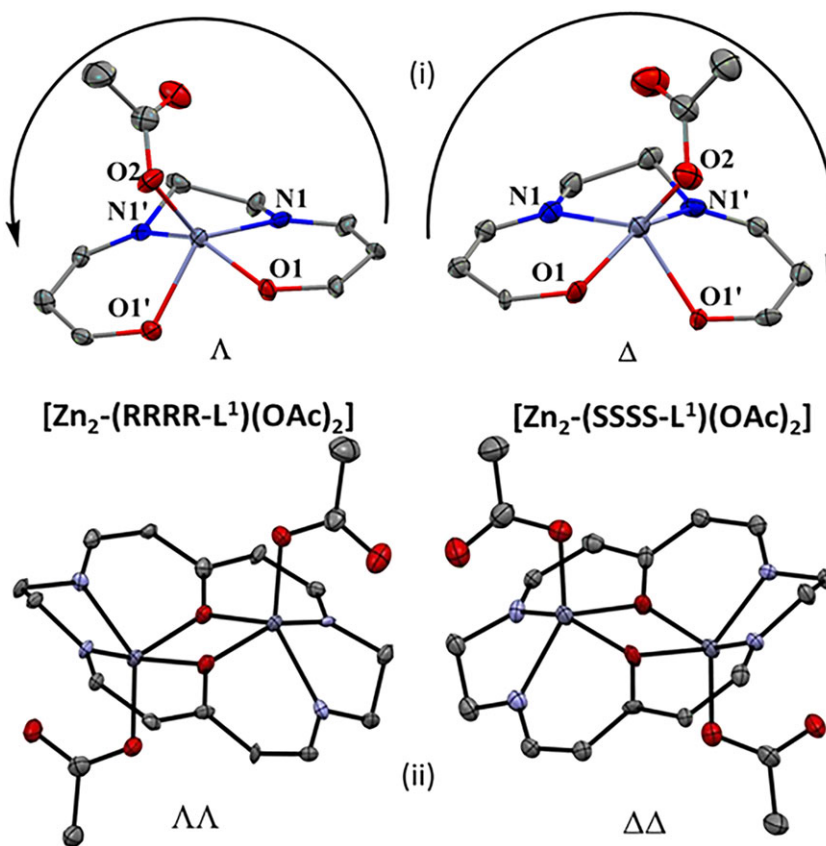


**FIGURE 3** Schematic representation of: (i)  $\Lambda$  and  $\Delta$  metal-centred chirality; (ii)  $\Lambda\Lambda$  in complex **1** and  $\Delta\Delta$  in complex **1'** (phenylmoieties are removed for clarity)

However, such descriptors are generally described for square-planar and octahedral complexes in the literature. Although the assignment is not that straightforward for pentacoordinated complexes, there are a good number of reports available in the literature.<sup>[20]</sup> The chromophoric arrangement of N<sub>2</sub>O<sub>3</sub> around the metal centre Zn1 and Zn2 is assigned as  $\Lambda$  and  $\Delta$  depending upon clockwise and counterclockwise rotation, as shown in Figure 3. The chromophore O1-N1-N1'-O1'-O2 of Zn2 and O1-N2-N2'-O1'-O3 around Zn1 revolve in the counterclockwise direction in complex **1**, in which the ligands possessing RRRR chiral carbon are assigned  $\Lambda\Lambda$  descriptor. Following this, complex **1'** having SSSS conformer of complex **1'** produces the  $\Delta\Delta$  enantiomer, as shown in Figure 3.

## 2.1 | Structural description by single-crystal X-ray diffraction

All these zinc (II) dimeric complexes were yellow in colour, and slow evaporation of their DCM/CH<sub>3</sub>CN solvent mixture provided a suitable single crystal for **1**, **1'** and **2'**. Summary of the crystallographic data for all the complexes are given in Table 1. The neutral binuclear zinc (II) complex consisting of two DPEN and two 4-MDFP units incorporates two Zn (II) metals. The DPEN used in the synthesis was of enantiopure form either in (*1R*, *2R*) or (*1S*, *2S*), the respective ligand thus gains four chiral centres in each complex.

The enantiopure dimeric complexes of zinc (II) acetate are crystallized in chiral space groups *P2*<sub>1</sub> in **1** and **1'** and

**TABLE 1** Summary of the crystal data for **1**, **1'** and **2'**

Identification code	(1)	(1')	(2')
Empirical formula	C <sub>56</sub> H <sub>54</sub> Cl <sub>4</sub> N <sub>6</sub> O <sub>6</sub> Zn <sub>2</sub>	C <sub>50</sub> H <sub>48</sub> N <sub>4</sub> O <sub>8</sub> Zn <sub>2</sub>	C <sub>56</sub> H <sub>57</sub> N <sub>4</sub> O <sub>6.5</sub> Zn <sub>2</sub>
Formula weight	1179.59	963.66	1020.79
Temp./K	100	100	100
Crystal size/mm <sup>3</sup>	0.16 × 0.16 × 0.12	0.24 × 0.18 × 0.12	0.18 × 0.12 × 0.12
Crystal system	monoclinic	monoclinic	orthorhombic
Space group	<i>P2</i> <sub>1</sub>	<i>P2</i> <sub>1</sub>	<i>P2</i> <sub>1</sub> <i>2</i> <sub>1</sub> <i>2</i> <sub>1</sub>
<i>a</i> /Å	11.2314(5)	12.4061(8)	10.6782(4)
<i>b</i> /Å	10.7745(4)	10.8649(7)	20.1147(8)
<i>c</i> /Å	22.2565(9)	16.7263(13)	24.4386(9)
$\alpha$ /°	90	90	90
$\beta$ /°	96.386(3)	101.323(5)	90
$\gamma$ /°	90	90	90
Volume/Å <sup>3</sup>	2676.61(19)	2210.7(3)	5249.1(3)
<i>Z</i>	2	2	4
$\rho_{\text{calc}}$ /cm <sup>3</sup>	1.464	1.448	1.292
$\mu$ /mm <sup>-1</sup>	1.152	1.146	0.967
<i>F</i> (000)	1216.0	1000.0	2132.0
Radiation	MoK $\alpha$ ( $\lambda$ = 0.71073)	MoK $\alpha$ ( $\lambda$ = 0.71073)	MoK $\alpha$ ( $\lambda$ = 0.71073)
Reflections collected	19 532	37 601	91 000
Independent reflections	8475 [ <i>R</i> <sub>int</sub> = 0.0514, <i>R</i> <sub><math>\sigma</math></sub> = 0.0868]	9058 [ <i>R</i> <sub>int</sub> = 0.0768, <i>R</i> <sub><math>\sigma</math></sub> = 0.0817]	10 753 [ <i>R</i> <sub>int</sub> = 0.0540, <i>R</i> <sub><math>\sigma</math></sub> = 0.0381]
Data/restraints/parameters	8475/33/601	9058/5/587	10 753/295/711
Goodness-of-fit on <i>F</i> <sup>2</sup>	1.045	1.027	1.040
Final <i>R</i> indexes [ <i>I</i> ≥ 2 $\sigma$ ( <i>I</i> )]	<i>R</i> <sub>1</sub> = 0.0645, <i>wR</i> <sub>2</sub> = 0.1618	<i>R</i> <sub>1</sub> = 0.0513, <i>wR</i> <sub>2</sub> = 0.1101	<i>R</i> <sub>1</sub> = 0.0323, <i>wR</i> <sub>2</sub> = 0.0707
Final <i>R</i> indexes [all data]	<i>R</i> <sub>1</sub> = 0.0903, <i>wR</i> <sub>2</sub> = 0.1794	<i>R</i> <sub>1</sub> = 0.0793, <i>wR</i> <sub>2</sub> = 0.1233	<i>R</i> <sub>1</sub> = 0.0420, <i>wR</i> <sub>2</sub> = 0.0738
Largest diff. peak/hole/e Å <sup>-3</sup>	1.16/−1.26	1.41/−0.52	0.38/−0.51
Flack parameter	0.006(13)	−0.032(10)	0.009(4)
CCDC	1867277	1867278	1867279

$P2_12_12_1$  in **2'** with two and four molecules in the unit cell, respectively. The selected bond distances and bond angles are presented in Figure S15 and Table S2. The macrocyclic ligand containing  $N_2O_2N_2$  metal-binding domain accommodates two Zn (II) ions. All the ligands in  $[Zn_2L^1(OAc)_2]$  to  $[Zn_2L^4(OAc)_2]$  possess two metal-binding domains, each containing  $N_2O_2$  chromophoric compartments with two azomethine nitrogens and two phenolic oxygens. The central phenolate oxygens (O1, O2) bridge both the Zn (II) centres and adopt a star-like conformation, as shown in Figures 4–6. Thus, each Zn (II) ion coordinating

to two azomethine nitrogens N1, N2 and two phenolate oxygens O1, O2 form a distorted square base, with the fifth coordination occupied by acetate ions in its axial site, revealing a distorted square-pyramidal geometry of Zn (II) metals in all the complexes.

The Zn (II) metal in **1** (Figure 4) sitting on the  $N_2O_2$  square base coordinated to N1N2O2O1 chromophoric atoms with bond distances Zn1-N1 = 2.043(8) Å, Zn1-N2 = 2.047(9) Å, Zn1-O1 = 1.996(8) Å and Zn1-O2 = 2.072(8) Å. The Zn1 is moved up slightly by 0.764 Å and the Zn2 is moved down by 0.767 Å from their respective

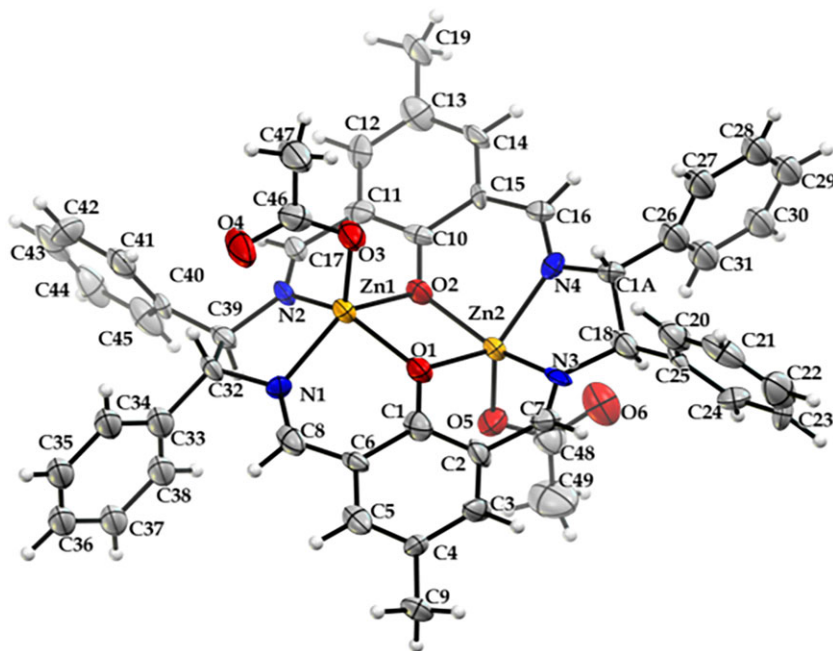


**FIGURE 4** ORTEP diagram of **1** showing atom numbering (solvents were removed for better clarity)

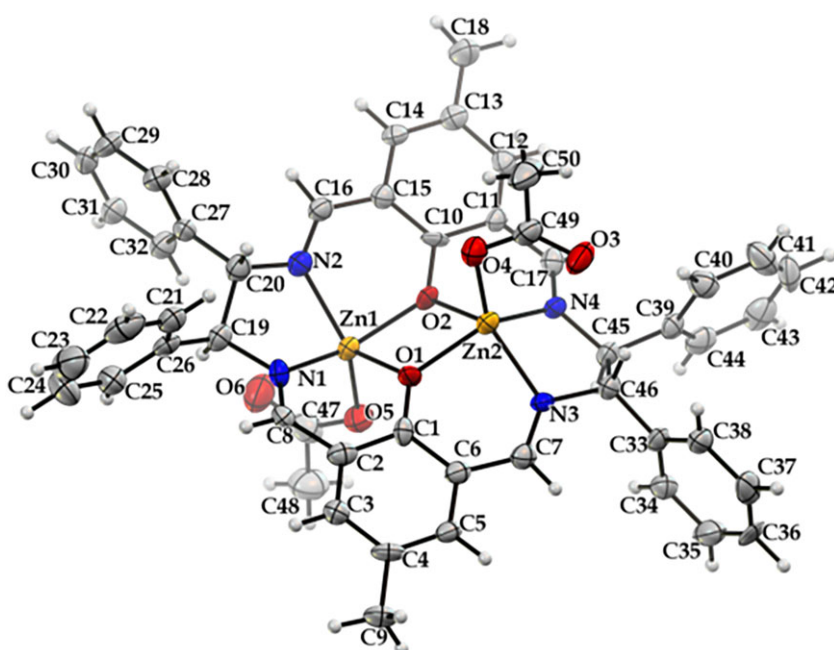


**FIGURE 5** ORTEP diagram of **1'** showing atom numbering (solvents were removed for better clarity)

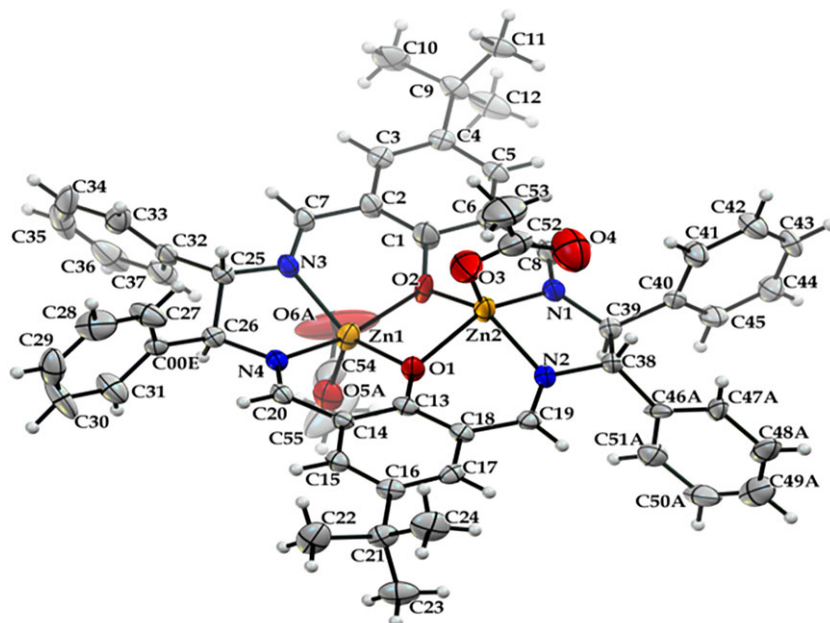


**FIGURE 6** ORTEP diagram of **2'** showing atom numbering (solvents were removed for better clarity)

mean plane. The Zn1-Zn2 distance within the dimer is measured as 3.167 Å. The *trans* angles  $\angle O2Zn1N1 = 131.8(3)^\circ$  and  $\angle O1Zn1N2 = 139.5(4)^\circ$ ; *cis* angles  $\angle N2Zn1O2$ ,  $\angle N2Zn1N1$ ,  $\angle O1Zn1O2$ ,  $\angle O1Zn1N1$  are found to be 80.9(3), 81.8(3), 76.7(3), 88.5(3)°.

The Zn (II) metal in **1'** (Figure 5) sitting on the  $N_2O_2$  square base coordinated to N1N2O2O1 atoms with bond distances Zn1-N1 = 2.051(6) Å, Zn1-N2 = 2.061(6) Å, Zn1-O1 = 2.076(5) Å and Zn1-O2 = 1.993(5) Å. The Zn1

ion is moved down slightly by 0.786 Å and the Zn2 is moved up by 0.779 Å from their respective mean planes. The Zn1-Zn2 distance is 3.170 Å. The *trans* angles  $\angle O2Zn1N1 = 147.7(2)^\circ$  and  $\angle O1Zn1N2 = 121.2(2)^\circ$ ; and the *cis* angles  $\angle N2Zn1O2$ ,  $\angle N2Zn1N1$ ,  $\angle O1Zn1O2$ ,  $\angle O1Zn1N1$  are found to be 86.7(2), 81.6(2), 78.07(19), 82.4(2)°.

The Zn (II) metal in **2'** (Figure 6) sitting on the  $N_2O_2$  square base coordinated to N1N2O2O1 atoms with bond distances Zn1-N3 = 2.085(3) Å, Zn1-N4 = 2.041(3) Å,

**TABLE 2** Screening of catalyst<sup>a</sup>

Entry	Catalyst	Catalyst, X mol%	Yield, <sup>b</sup> %	ee, <sup>c</sup> %
1	1	5	75	65(1 <i>S</i> ,2 <i>R</i> )
2	1'	5	73	64(1 <i>R</i> ,2 <i>S</i> )
3	2	5	74	60(1 <i>S</i> ,2 <i>R</i> )
4	2'	5	75	61(1 <i>R</i> ,2 <i>S</i> )
5	1	2	65	50
6	1	8	75	69
7	1	10	80	75
8	1	15	85	70
9	1	20	80	66

<sup>a</sup>All the reactions were carried out with 0.2 mmol of mesohydrobenzoin, 0.2 mmol of PhCOCl, 0.4 mmol of lutidine and 2 ml of solvent.

<sup>b</sup>Isolated yield.

<sup>c</sup>Determined by HPLC (Lux cellulose-1 column). Reaction time 12 hr.

Zn1-O1 = 2.030(2) Å and Zn1-O2 = 1.939(8) Å. The Zn1 and Zn2 atoms in the dimer with an intradimer M-M distance 3.185 Å are moved down slightly by 0.686 Å (Zn1) and up by 0.859 Å (Zn2), respectively, from their respective mean planes towards their fifth axial coordination. The *trans* angles  $\angle$ O2Zn1N4 = 144.0(4)° and  $\angle$ O1Zn1N3 = 136.85(10)°, and the *cis* angles  $\angle$ O2Zn1N3, N4Zn1N3, O1Zn1O2, O1Zn1N4 are found to be 88.8(2), 81.41(10), 75.48(15), 86.18(9)°. In all these cases, the phenolate oxygen bridging both the metal centres provides a  $\mu_2$ -phenoxo bridge. Having used an enantiopure 1,2-diphenylethylenediamine, the respective complexes in their crystallographic structures illustrate a  $\Lambda\Lambda$  configuration in **1** and **2**, and a  $\Delta\Delta$  metal-centred chirality in **1'** and **2'**. After the successful synthesis of these complexes, their enantiopurity inspired us to investigate their catalytic ability in converting meso-hydrobenzoin **3a** to corresponding monobenzoylated products (1*S*,2*R*)-**3b** and (1*R*,2*S*)-**3b**, and the respective data are shown in Table 2.

Initially, we tested all the catalysts (**1**, **1'**, **2** and **2'**) with 5 mol% catalyst loading, 0.5 equivalence of lutidine, using benzoyl chloride (PhCOCl, 0.5 eq.) as acylating agent and dichloroethane as a solvent at room temperature (RT; Table 2, entries 1–4). The reaction time was monitored by thin-layer chromatography (TLC) following the consumption of the substrate. All the catalysts gave  $74 \pm 1\%$  yields and *ee* ranges of 60–65% (Table 2, entries 1–4). The catalysts **1** and **1'** gave similar yields, they varied only in the enantiomeric nature of the product of the monoesters. Among the four catalysts screened, the catalysts **1** and **1'** showed an enhancement in the enantioselectivity that encouraged us to consider them for further optimization. Because both these catalysts gave similar yields and enantioselectivity, complex **1** was chosen for further optimization. Initially, we attempted to vary the amount of catalyst from 2 to 20 mol% (Table 2, entries 5–9). When the catalyst amount increased from 2 mol% to 10 mol%, the yield also increased from 65% to 80% (Table 2, entries 7–9) alongwith *ee* (50–75%). A further increment in the catalyst loading from 15 mol% to 20 mol% caused a dramatic decrease in the enantioselectivity, i.e. 70–66% (Table 2, entries 8 and 9). Henceforth, we decided to fix the amount of catalyst as 10 mol%, in which the yield was obtained as 80% with highest *ee* 75% (Table 2, entry 7). Then, in an attempt to optimize the temperature, the yield and *ee* were monitored at different temperatures, for example 40°C, 0°C, –5°C, and up to –10°C (Figure 7a). While increasing the temperature from RT (30°C) to 40°C, a significant loss in the enantioselectivity to 45% and yield to 70% (Figure 7a) was observed. Hence, lowering the temperature from RT to 0°C gave an enhancement, i.e. yield 85%, *ee* 78% (Figure 7a). A similar approach at –5°C gave 86% yield, but the fall in *ee* to 63%

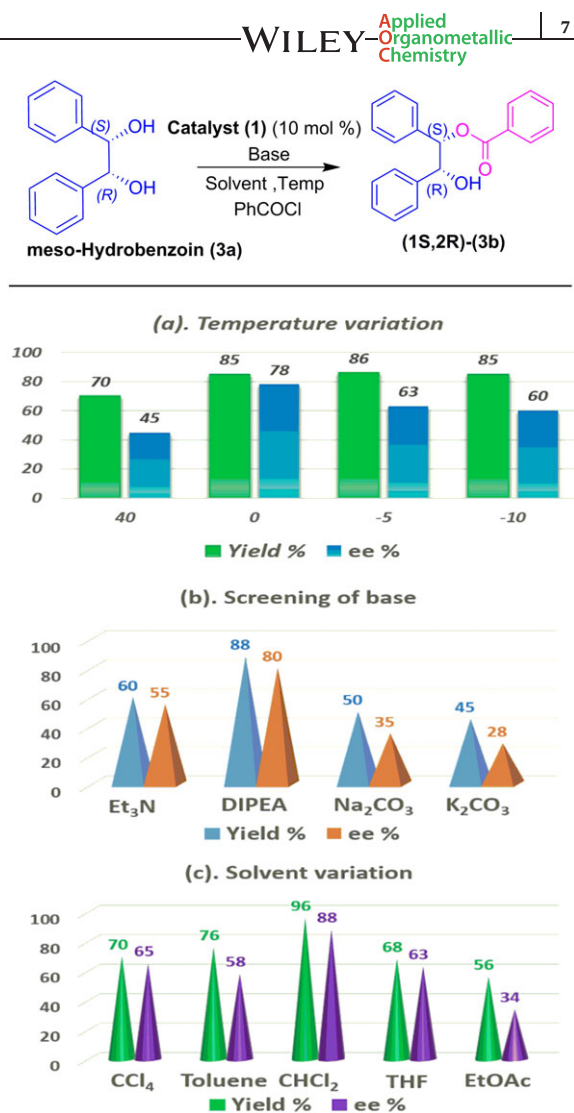


**FIGURE 7** Optimization of reaction conditions. (a) All the reactions were carried out with 10 mol% of catalyst, 0.2 mmol of mesohydrobenzoin, 0.2 mmol of PhCOCl, 0.4 mmol of base and 2 ml of solvent. (b) Isolated yield. (c) Determined by high-performance liquid chromatography (HPLC; Lux cellulose-1 column). (d) Reaction time is 12 hr

(Figure 7a) was not encouraging. A further decrease in temperature to –10°C resulted in 85% yield with a further fall in the *ee* to 60% (Figure 7a). Thus, it is convincing that to obtain a better yield and *ee*, the temperature of 0°C has been chosen as an optimum temperature for this reaction. As the yield and enantioselectivity of the product depends on the strength of the base, an attempt to identify the optimum base was also performed. Our initial analysis without using base provides a very negligible amount of yield. Hence, we have conducted the reaction using a variety of bases, such as triethylamine (Et<sub>3</sub>N; Figure 7b; yield 60%, *ee* 55%), diisopropylethylamine (DIPEA; Figure 7b; yield 88%, *ee* 80%) and some inorganic bases like Na<sub>2</sub>CO<sub>3</sub> (Figure 7b; yield 50%, *ee* 35%) or K<sub>2</sub>CO<sub>3</sub> (Figure 7b; yield 45%, *ee* 28%). All these bases act as deprotonating agents; among the bases used,

DIPEA gives better results than the others. Hence, DIPEA was chosen as the best deprotonating agent. Similarly, solvent plays a major role in homogeneous catalysis, so we next examined for a suitable solvent. As most of the reported benzoylation reactions are conducted in halogenated solvents, the main emphasis was given for halogenated solvents, and the results are presented in Figure 7c. Solvents such as  $\text{CCl}_4$  (Figure 7c; yield 70%, *ee* 65%), DCM (Figure 7c; yield 96%, *ee* 88%) and a few non-halogenated solvents such as toluene (Figure 7c; yield 76%, *ee* 58%), THF (Figure 7c; yield 68%, *ee* 63%) and EtOAc (Figure 7c; yield 56%, *ee* 34%) were tested. Excitingly, DCM gave a good yield of 96% and better enantioselectivity of 88%.

Adapting the above-optimized conditions, we next investigated various meso-1,2-diols as substrates (Figure 8, **3b–13b**) using **1** as a catalyst. In the case of **3a**, the catalyst gave 96% yield with 88% *ee* (Figure 8, **3b**). Then we moved from acyclic diol to cyclic diol containing five-membered and eight-membered rings. The cyclopentane diol (**4a**) has converted to the respective monoester (**4b**) with 92% yield and 40% *ee* (Figure 8, **4b**), the cyclohexane diol (**5a**)

produced monoester (**5b**) with 91% yield and 50% *ee* (Figure 8, **5b**).

The cyclooctane diol **6a** gave 93% yield and 40% *ee* of monoester product **6b** (Figure 8; **6b**). The 2,3-butane-diol **7a**, which is a methyl-substituted diol, gave good yield (90%) but the *ee* was very poor, i.e. 30% (Figure 8, **7b**). From the substrate variation, the mesohydrobenzoin (**3a**) gave the best result (yield 96%, *ee* 88%) compared with the other substrates (Figure 8, **3b**). This may be because the 1,2-diphenyl moiety with a phenyl ring had a strong  $\pi \dots \pi$  interaction between the catalyst and substrates with aromatic moiety that might have favoured the asymmetric benzoylation. Hence, keeping mesohydrobenzoin as a substrate, we then varied different acyl and aroyl chlorides with the same optimized conditions, and the results are presented in Figure 8, **8b–13b**. When 4-methylbenzoylchloride **8a** was used, the corresponding monoester **8b** was produced with 90% yield and 78% *ee* (Figure 8, **8b**). The 4-nitrobenzoylchloride **9a** gave monoester **9b** with 96% yield, but the enantioselectivity was reduced to 20% (Figure 8, **9b**), this may be because the bulky nitro group at the para-position might interrupt

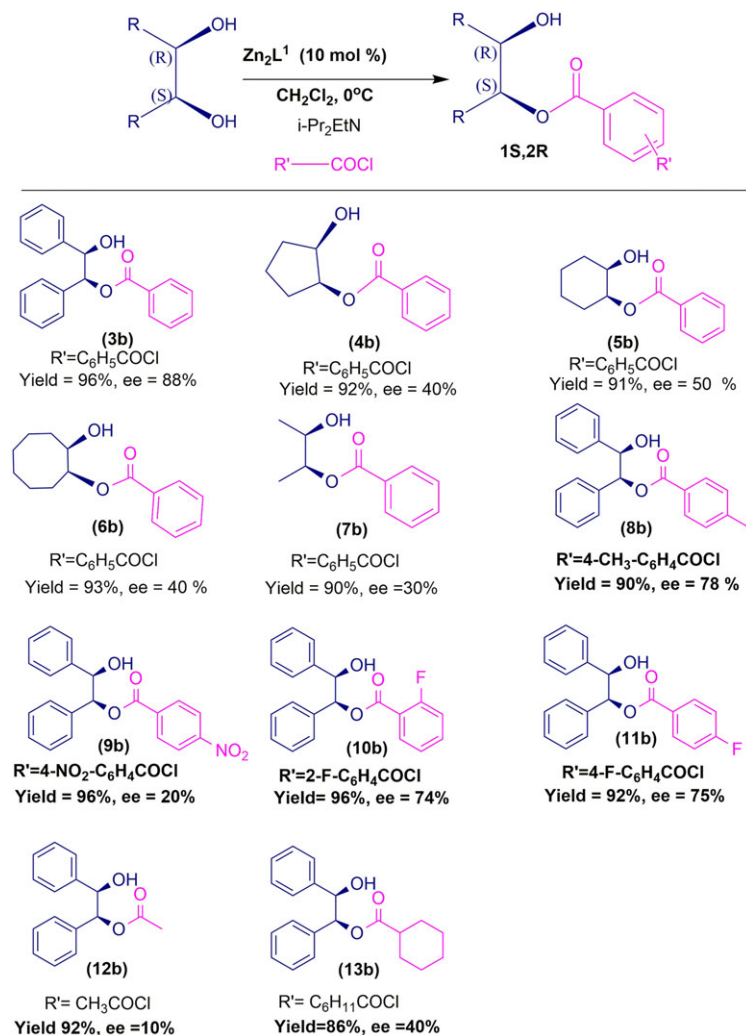


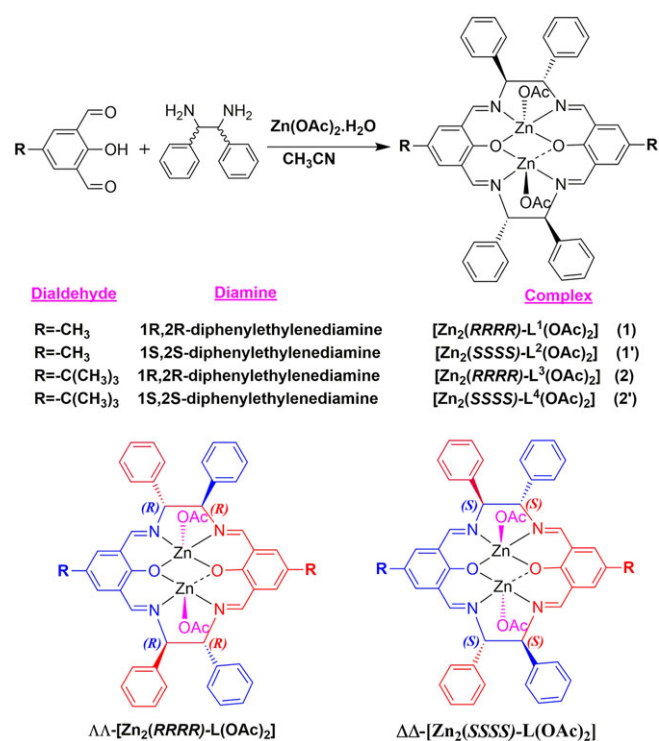
**FIGURE 8** Asymmetric benzoylation of meso-1,2-diol with various aroyl and acylchloride. (a) All the reactions were carried out with 10 mol% of catalyst, 0.2 mmol of substrates, 0.2 mmol of PhCOCl, 0.4 mmol of DIPEA and 2 ml of solvent. (b) Isolated yield. (c) Determined by high-performance liquid chromatography (HPLC; Lux cellulose-1 column). (d) Reaction time is 12 hr

the catalyst–substrate interactions. The remaining 2-fluorobenzoyl-chloride **10a** and 4-fluorobenzoylchloride **11a** gave good yield (96% and 92%, respectively) and *ee* (74% and 75%, respectively; Figure 8, **10b** and **11b**). The aroyl chlorides thus gave encouraging results, so we then screened non-aroyl acyclic (acetyl chloride, **12a**) and cyclic chlorides (cyclohexanecarbonyl chloride, **13a**) that are found to produce monoesters (**12b** and **13b**) with enhanced yield (92% and 86%, respectively) but a dramatic decrease in *ee* (10% and 40%, respectively; Figure 8, **12b** and **13b**). These two non-aroyl chlorides thus produced a good yield but poor enantioselectivity. The variation on the acylating agent suggests that the unsubstituted benzoyl chloride (Figure 8, **3b**) is a better acylating agent compared with the others.

Based on the results, we proposed a probable mechanism for the desymmetrization of meso diol (Scheme 2). In the first step, the substrate interacted with the catalyst at a vacant site opposite the acetyl group attached in the metal for an octahedral complex (TS-I), then the alcoholic proton deprotonated by DIPEA interacted with benzoyl chloride (TS-II) to form a stereoselective monoester. High stereoselectivity was observed only in mesohydrobenzoin compared with the other diols. The phenyl moiety in the mesohydrobenzoin had a strong  $\pi \dots \pi$  interaction with the catalyst, leading to the formation of the stereoselective product. Although the Zn–Zn intermetallic distance in all

three complexes ranged from 3.167 Å to 3.185 Å, similar to that observed in the dimeric zinc reported<sup>[16,21]</sup> (Zn–Zn = 3.178 Å), the present complex in its chiral space group differs in its desymmetrization mechanism. The binuclear complex possessed  $\Lambda\Lambda$  or  $\Delta\Delta$  homochiral geometry in the dimeric association, and each Zn (II) centre possessed a pentacoordinated geometry. Hence, we propose that there is no possibility for the bidentate or chelate coordination of the diol with the Zn (II) dimeric centres in the present complexes. Instead, one of the two hydroxyl groups of the diol might have selectively coordinated through the sixth coordination site in a monodentate fashion with each Zn (II) centre, while the other hydroxyl group remained undisturbed. Thus, the non-superimposable  $\Lambda\Lambda$  chirality in the dimer does not permit the diol to establish bimetallic coordination from the same side. Hence, each Zn (II) centre in the homochiral dimer selectively binds one of the two hydroxyls of the diol and establishes a sixth coordination site from the opposite side, and thus both the Zn (II) centres in their homochiral nature promote a stereoselective product. To support this mechanism, we used <sup>1</sup>H-NMR to monitor a model experiment that followed successive additions of mesohydrobenzoin, DIPEA and benzoylchloride and catalyst (i)  $[\text{Zn}_2(\text{RRRR-L}^1)(\text{OAc})_2]$ ; (ii)  $[\text{Zn}_2(\text{RRRR-L}^1)(\text{OAc})_2]$  + mesohydrobenzoin; (iii)  $[\text{Zn}_2(\text{RRRR-L}^1)(\text{OAc})_2]$  + mesohydrobenzoin + DIPEA; and (iv)  $[\text{Zn}_2(\text{RRRR-L}^1)(\text{OAc})_2]$  + mesohydrobenzoin + DIPEA + benzoyl chloride. The <sup>1</sup>H-NMR for all these experiments (Figure S18) and the follow-up analysis strongly reconfirm the above-proposed mechanism.

The recyclability of the catalyst was tested to understand its efficiency. Adapting **1**, the mesohydrobenzoin was chosen as a substrate and benzoyl chloride as acylating agent at optimized reaction conditions. The yield and *ee* were monitored for up to six cycles, and the respective data are shown in Figure 9. Interestingly, the catalyst was found to be efficient by showing no loss of enantioselectivity and yield up to the sixth cycle. The recycled catalyst was checked by Fourier transform-infrared (FT-IR) spectra. Encouragingly, the spectra clearly matching with the fresh catalyst, suggest that even after six cycles the catalyst is stable (Figure S19).



**SCHEME 2** Proposed mechanism for the desymmetrization of meso diol by catalyst **1**

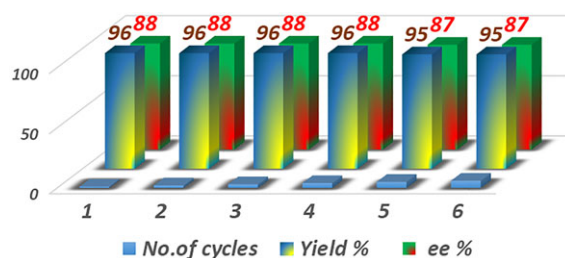


**FIGURE 9** The recyclability of the catalyst **1** mesohydrobenzoin with benzoyl chloride in optimized conditions

### 3 | CONCLUSIONS

In conclusion, we report here the synthesis of a series of important macrocyclic binuclear Zn (II) complexes that are easy-to-synthesize and enantiopure. These binuclear complexes are demonstrated as efficient catalysts for selective desymmetrization of  $C_2$ -symmetric meso diols to unsymmetrical monoesters with good yield and rich enantioselectivity (96% yield and 88% ee). The Zn (II) geometry has  $\Delta\Delta$  and  $\Lambda\Lambda$  metal-centred chirality, where each centre in the dimeric unit is involved efficiently in desymmetrizing the meso diols, which is otherwise highly challenging. The intermetallic distance derived from the crystal structure of the complexes **1**, **1'** and **2'** and the homochiral nature  $\Lambda\Lambda$  or  $\Delta\Delta$  at the geometry involves efficiently promoting enantioselective product is evident without any ambiguity. The catalyst has been successfully recycled up to six cycles without any significant loss in its activity.

### 4 | EXPERIMENTAL

#### 4.1 | Materials and methods

2-Hydroxy-5-methyl-1,3-benzenedicarboxaldehyde, 4-*tert*-butyl-2,6-diformylphenol, (*1R,2R*)-diphenylethylenediamine, (*1S,2S*)-diphenylethylenediamine and zinc acetate dihydrate were purchased from Aldrich. All the chemicals were used as received without any further purification. Microanalyses were performed by using a Perkin-Elmer PE 2400 series-II CHNS/O elemental analyser. IR spectra were recorded using KBr pellets (1% w/w) on a Perkin-Elmer Spectrum GX FT-IR spectrophotometer. Electronic spectra were recorded on a Shimadzu UV 3101 PC spectrophotometer. Mass analyses were performed using the positive electron spray ionization (ESI<sup>+</sup>) technique on water Q TOF-micro mass spectrometer. <sup>1</sup>H-NMR spectra were recorded on a Bruker *Avance* DPX 200, 500 MHz and JEOL Delta 600 MHz FT-NMR spectrometer. Chemical shifts for proton resonances are reported in ppm ( $\delta$ ) relative to tetramethylsilane. The CD spectra were recorded on a JASCO 815 spectrometer. Suitable crystals for complex **1**, **1'** and **2'** were selected and mounted on a Mitegen mesh with paratone oil. Data were collected at 100 K on a Bruker Kappa APEX2 CCD diffractometer with Mo-K $\alpha$  radiation. Preliminary lattice parameters and orientation matrices were obtained from three sets of frames. Then full data were collected using the  $\omega$  and  $\phi$  scan method with a frame width of 0.5°. The enantioselectivity of the monobenzoylated product was determined by high-performance liquid chromatography

(HPLC; Shimadzu SCL-10AVP) using chiral columns (Phenomenex Lux cellulose-1 and Amylose-2 columns).

#### 4.2 | Synthesis

Acetonitrile (5 ml) solution of the 2-hydroxy-5-methyl-1,3-benzenedicarboxaldehyde (16.4 mg, 0.1 mmol in **L**<sup>1</sup> and **L**<sup>2</sup>) or 4-*tert*-butyl-2,6-diformylphenol (20.6 mg, 0.1 mmol, in **L**<sup>2</sup> and **L**<sup>3</sup>), triethylamine (14  $\mu$ l, 0.1 mmol) and zinc acetate dihydrate (21.9 mg, 0.1 mmol) were mixed together and constantly stirred at RT for 15 min. To this, acetonitrile solution of (*1R,2R*)- or (*1S,2S*)-diphenylethylenediamine (21.2 mg, 0.1 mmol) was added drop by drop. After the complete addition of diamine, the reaction mixture was constantly stirred for 6 hr. A colour change from pale yellow to an intense yellow was observed. Finally, the solvent was removed by rotavapor and the resulting residue was washed with dichloromethane (50 ml) and water (3  $\times$  10 ml), the organic layer was separated and treated with anhydrous sodium sulphate and recrystallized from the DCM/acetonitrile (v/v) mixture to yellow polycrystalline products.

##### 4.2.1 | [**Zn**<sub>2</sub>(**RRRR**)-**L**<sup>1</sup>(**OAc**)<sub>2</sub>] (**1**)

C<sub>50</sub>H<sub>44</sub>N<sub>4</sub>O<sub>6</sub>Zn<sub>2</sub>. Yield 80%, UV-Vis.  $\lambda_{\max}/\text{nm}$  ( $\epsilon/\text{dm}^3 \text{ mol}^{-1} \text{ cm}^{-1}$ ): 256 (109 523), 381 (42 078). FT-IR (KBr):  $\nu = 3446, 2924, 1630, 1384, 1326, 1232, 1121, 1000, 740, 701 \text{ cm}^{-1}$ . MS (ESI<sup>+</sup>):  $m/z$  calcd for [M (CH<sub>3</sub>OH)·(H<sub>2</sub>O)] + H<sup>+</sup>, [C<sub>51</sub>H<sub>51</sub>N<sub>4</sub>O<sub>8</sub>Zn<sub>2</sub>]<sup>+</sup>, 977.23; found: 977.68. <sup>1</sup>H-NMR (DMSO-*d*<sub>6</sub>, 600 MHz,  $\delta$ , ppm): 8.25 (s, 2H, CH=N), 8.05(s, 2H, CH=N), 7.40 (m, 5H, Ar), 7.35–7.37 (m, 11H, Ar), 7.31–7.33 (m, 8H, Ar), 5.44(s, 2H, Ph\*CHN), 5.27 (s, 2H, Ph\*CHN), 2.14 (s, 3H, CH<sub>3</sub>). Elemental analysis: chemical formula; C<sub>50</sub>H<sub>48</sub>N<sub>4</sub>O<sub>8</sub>Zn<sub>2</sub>, calcd (found): C, 62.32 (62.44); H, 5.02 (4.76); N, 5.81 (5.56) %.

##### 4.2.2 | [**Zn**<sub>2</sub>(**SSSS**)-**L**<sup>2</sup>(**OAc**)<sub>2</sub>] (**1'**)

C<sub>62</sub>H<sub>52</sub>N<sub>4</sub>O<sub>10</sub>Zn<sub>2</sub>. Yield 80%. UV-Vis.  $\lambda_{\max}/\text{nm}$  ( $\epsilon/\text{dm}^3 \text{ mol}^{-1} \text{ cm}^{-1}$ ): 256 (74 624), 380 (25 996). FT-IR (KBr):  $\nu = 3418, 2835, 1631, 1594, 1384, 1352, 1118, 1002, 762, 701, 618 \text{ cm}^{-1}$ . MS (ESI<sup>+</sup>):  $m/z$  calcd for [M-OAc]<sup>+</sup>, C<sub>48</sub>H<sub>41</sub>N<sub>4</sub>O<sub>4</sub>Zn<sub>2</sub>, 867.17; found: 867.99. <sup>1</sup>H-NMR (DMSO-*d*<sub>6</sub>, 600 MHz,  $\delta$ , ppm): 8.20 (s, 2H, CH=N), 8.00 (s, 2H, CH=N), 7.36 (m, 5H, Ar), 7.33–7.31 (m, 11H, Ar), 7.30–7.28 (m, 8H, Ar), 5.38 (s, 2H, Ph\*CHN), 5.21 (s, 2H, Ph\*CHN), 2.10 (s, 3H, CH<sub>3</sub>). Elemental analysis: chemical formula: C<sub>50</sub>H<sub>50</sub>N<sub>4</sub>O<sub>9</sub>Zn<sub>2</sub>, calcd (found): C, 61.17 (61.36); H, 5.13 (5.46); N, 5.71 (5.34) %.

### 4.2.3 | [Zn<sub>2</sub>(RRRR)-L<sup>3</sup>(OAc)<sub>2</sub>] (2)

C<sub>68</sub>H<sub>60</sub>N<sub>4</sub>O<sub>8</sub>Zn<sub>2</sub>. Yield 82%. UV-Vis. λ<sub>max</sub>/nm (ε/dm<sup>3</sup> mol<sup>-1</sup> cm<sup>-1</sup>): 257 (133 840), 375 (501 673). FT-IR (KBr): ν = 3416, 2815, 2721, 1629, 1595, 1384, 1339, 1124, 767, 617 cm<sup>-1</sup>. MS (ESI)<sup>+</sup>: m/z calcd for [M-OAc]<sup>+</sup>, C<sub>54</sub>H<sub>53</sub>N<sub>4</sub>O<sub>4</sub>Zn<sub>2</sub>, 951.26; found: 951.11. <sup>1</sup>H-NMR (DMSO-*d*<sub>6</sub>, 600 MHz, δ, ppm): 1.20 (s, 18H, -C (CH<sub>3</sub>)<sub>3</sub>), 5.17 (s, 2H, Ph\*CHN), 5.46 (s, 2H, Ph\*CHN), 7.30–7.32 (m, 4H, Ar), 7.35–7.37 (m, 8H, Ar), 7.42–7.43 (m, 8H, Ar), 7.57 (s, 4H, Ar), 8.25 (s, 2H, CH=N), 8.42 (s, 2H, CH=N). Elemental analysis: chemical formula: C<sub>58</sub>H<sub>63</sub>N<sub>5</sub>O<sub>8</sub>Zn<sub>2</sub>, calcd (found): C, 63.97 (63.78); H, 5.83 (4.7); N, 6.43 (6.18) %.

### 4.2.4 | [Zn<sub>2</sub>(SSSS)-L<sup>4</sup>(OAc)<sub>2</sub>] (2')

C<sub>68</sub>H<sub>60</sub>N<sub>4</sub>O<sub>8</sub>Zn<sub>2</sub>. Yield 82%. UV-Vis. λ<sub>max</sub>/nm (ε/dm<sup>3</sup> mol<sup>-1</sup> cm<sup>-1</sup>): 257 (89 011), 375 (29 739). FT-IR (KBr): ν = 3413, 2812, 2807, 2729, 1632, 1590, 1384, 1123, 765, 702, 616 cm<sup>-1</sup>. MS (ESI)<sup>+</sup>: m/z calcd for [M-OAc]<sup>+</sup>, C<sub>54</sub>H<sub>53</sub>N<sub>4</sub>O<sub>4</sub>Zn<sub>2</sub>, 951.26; found: 951.44. <sup>1</sup>H-NMR (DMSO-*d*<sub>6</sub>, 600 MHz, δ, ppm): 1.19 (s, 18H, -C (CH<sub>3</sub>)<sub>3</sub>), 1.64 (s, 6H, CH<sub>3</sub>COO), 5.14 (s, 2H, Ph\*CHN), 5.73 (s, 2H, Ph\*CHN), 7.29–7.30 (m, 4H, Ar), 7.33–7.35 (m, 12H, Ar), 7.49 (m, 8H, Ar), 8.13 (s, 2H, CH=N), 8.28 (s, 2H, CH=N). Elemental analysis: chemical formula: C<sub>56</sub>H<sub>62</sub>N<sub>4</sub>O<sub>9</sub>Zn<sub>2</sub>, calcd (found): C, 63.10 (63.66); H, 5.86 (5.47); N, 5.26 (5.92) %.

## 4.3 | General procedure for desymmetrization of meso diol

A dry and nitrogen-flushed 5-ml flask, equipped with a magnetic stirring bar, was charged with zinc (II) catalyst (10 mol%) and freshly distilled dry DCM (2 ml). Corresponding diol (0.2 mmol) and 2 equivalence DIPEA (0.4 mmol) were then added successively, and the resulting mixture was stirred for up to 10–15 min, and benzoyl chloride (0.2 mmol) was added slowly by syringe at 0°C. The mixture was stirred at the same temperature till the completion of the reaction. The reaction was monitored by TLC. After completion of the reaction, the solvent was evaporated by rotavapor and washed with hexane/ethyl acetate (95/5, v/v; four times) to separate the catalyst from the mixture. Finally, the crude product was purified by column chromatography (silica gel, 100–200 mesh using ethyl acetate and hexanes) to give the corresponding monoester product. Enantiomeric excess was determined by UFLC using Phenomenox Lux cellulose-1 and Amylose-2 columns using isopropanol and hexane as eluting agents. The absolute configurations

of the products were assigned by comparison of HPLC profiles with reported literature.<sup>[22]</sup>

## ACKNOWLEDGEMENTS

CSMCRI communication number CSIR-CSMCRI-162/2018. The authors gratefully acknowledge DST-SERB New Delhi (Project nos SR/S1/IC-23/2011 and SB/S1/IC-26/2013) for funding. The authors EC and RA acknowledge for CSIR-SRF grand. Members of Analytical Division & Centralized Instruments Facility (ADCIF) of CSIR-CSMCRI are acknowledged for their instrumentation support.

## ORCID

Palani S. Subramanian  <https://orcid.org/0000-0002-9035-0973>

## REFERENCES

- [1] R. N. Patel, A. Banerjee, Y. R. Pendri, J. Liang, C.-P. Chen, R. Mueller, *Tetrahedron: Asymmetry* **2006**, *17*, 175.
- [2] R. Mehvar, *J. Pharm. Pharmaceut. Sci.* **2001**, *4*, 185.
- [3] a) J. Ichikawa, M. Asami, T. Mukaiyama, *Chem. Lett.* **1984**, *13*, 949. b) T. Mukaiyama, I. Tomioka, M. Shimizu, *Chem. Lett.* **1984**, *13*, 49; c) Á. E. García, E. P. Kündig, *Chem. Soc. Rev.* **2012**, *41*, 7803.
- [4] F. Theil, *Catal. Today* **1994**, *22*, 517.
- [5] a) K. Ishihara, M. Kubota, H. Yamamoto, *Synlett* **1994**, *1994*, 611; b) T. Oriyama, K. Imai, T. Hosoya, T. Sano, *Tetrahedron Lett.* **1998**, *39*, 397 c) L. Duhamel, T. Herman, *Tetrahedron Lett.* **1985**, *26*, 3099.
- [6] a) F. Iwasaki, T. Maki, O. Onomura, W. Nakashima, Y. Matsumura, *J. Org. Chem.* **2000**, *65*, 996; b) D. Nanni, D. P. Curran, *Tetrahedron: Asymmetry* **1996**, *7*, 2418.
- [7] a) E. Vedejs, O. Daugulis, S. T. Diver, *J. Org. Chem.* **1996**, *61*, 430 b) E. Vedejs, O. Daugulis, N. Tuttle, *J. Org. Chem.* **2004**, *69*, 1389; c) J. Holz, O. Zayas, H. Jiao, W. Baumann, A. Spannenberg, A. Monsees, T. H. Riermeier, J. Almena, R. Kadyrov, A. Boerner, *Chem. Eur. J.* **2006**, *12*, 5001; d) L. Boren, K. Leijondahl, J.-E. Baeckvall, *Tetrahedron Lett.* **2009**, *50*, 3237.
- [8] a) S. Mizuta, M. Sadamori, T. Fujimoto, I. Yamamoto, *Angew. Chem., Int. Ed.* **2003**, *42*, 3383; b) S. Mizuta, T. Tsuzuki, T. Fujimoto, I. Yamamoto, *Org. Lett.* **2005**, *7*, 3633; c) H. Aida, K. Mori, Y. Yamaguchi, S. Mizuta, T. Moriyama, I. Yamamoto, T. Fujimoto, *Org. Lett.* **2012**, *14*, 812.
- [9] M. Candy, G. Audran, H. Bienaymé, C. Bressy, J. M. Pons, *Org. Lett.* **2009**, *11*, 4950.
- [10] a) E. Santaniello, P. Ferraboschi, P. Grisenti, A. Manzocchi, *Chem. Rev.* **1992**, *92*, 1071; b) J. Otera, *Chem. Rev.* **1993**, *93*, 1449. c) J. B. Jones, *Tetrahedron* **1986**, *42*, 3351; d) Z. F. Xie, H. Suemune, K. Sakai, *J. Chem. Soc. Chem. Commun.* **1987**, 838; e) A. C. Spivey, S. Arseniyadis, *Top. Curr. Chem.* **2010**, *291*, 233; f) C. E. Müller, P. R. Schreiner, *Angew. Chem. Int.*

- Ed.* **2010**, *50*, 6012; g) P. Somfai, *Angew. Chem. Int. Ed.* **1997**, *36*, 2731.
- [11] a) S. Nagumo, T. Arai, H. Akita, *Tetrahedron Lett.* **1997**, *38*, 5165; b) H. C. Kim, J.-H. Youn, S. H. Kang, *Synlett* **2008**, 2526.
- [12] T. Suzuki, *Tetrahedron Lett.* **2017**, *58*, 4731.
- [13] a) A. R. Silva, L. Carneiro, A. P. Carvalho, J. Pires, *Catal. Sci. Technol.* **2013**, *3*, 2415; b) L. Carneiro, A. R. Silva, P. S. Shuttleworth, V. Budarin, J. H. Clark, *Molecules* **2014**, *19*(8), 11 988.
- [14] a) N. Maignot, J. P. Mazaleyrat, *Synthesis* **1985**, 317; b) F. Iwasaki, T. Maki, W. Nakashima, O. Onomura, Y. Matsumura, *Org. Lett.* **1999**, *1*, 969.
- [15] a) B. M. Trost, T. Mino, *J. Am. Chem. Soc.* **2003**, *125*, 2410; b) B. M. Trost, S. Malhotra, T. Mino, N. S. Rajapaksa, *Chem. Eur. J.* **2008**, *14*, 7648; c) B. M. Trost, V. S. Chan, D. Yamamoto, *J. Am. Chem. Soc.* **2010**, *132*, 5186.
- [16] E. Chinnaraja, R. Arunachalam, M. K. Choudhary, R. I. Kureshy, P. S. Subramanian, *Appl. Organometal. Chem.* **2016**, *30*, 95.
- [17] E. Chinnaraja, R. Arunachalam, P. S. Subramanian, *ChemistrySelect* **2016**, *1*, 5331.
- [18] a) J. Crassous, *Chem. Soc. Rev.* **2009**, *38*, 830; b) N. Ousaka, Y. Takeyama, H. Iida, E. Yashima, *Nat. Chem.* **2011**, *3*, 856.; c) C. He, Y. Zhao, D. Guo, Z. Lin, C. Duan, *Eur. J. Inorg. Chem.* **2007**, 3451; d) M. Albrecht, S. Dehn, G. Raabe, R. Frohlich, *Chem. Commun.* **2005**, 5690; e) J. Crassous, *Chem. Commun.* **2012**, *48*, 9687; f) U. Knof, A. V. Zelewsky, *Angew Chem. Int. Ed.* **1999**, *38*, 302; g) M. Fujiki, *Symmetry* **2014**(6), 677 h) H. Ito, H. Tsukube, S. Shinoda, *Chem. Commun.* **2012**, *48*, 10 954; i) S. Zahn, J. W. Canary, *Science* **2000**, *288*, 1404; j) E. C. Constable, G. Zhang, C. E. Housecroft, M. Neuburger, J. A. Zampese, *Eur. J. Inorg. Chem.* **2010**, 2000; k) T. Maeda, Y. Furusho, M. Shiro, T. Takata, *Chirality* **2006**, *18*, 691.
- [19] a) J. Gao, J. H. Reibenspies, R. A. Zingaro, F. R. Wooley, A. E. Martell, A. Clearfield, *Inorg. Chem.* **2005**, *44*, 232; b) J. Gao, J. H. Reibenspies, A. E. Martell, *Angew. Chem. Int. Ed.* **2003**, *42*, 6008.
- [20] a) M. Seitz, S. Stempfhuber, M. Zabel, M. Schütz, O. Reiser, *Angew Chem. Int. Ed.* **2005**, *44*, 242; b) H. Miyasaka, S. Okamura, T. Nakashima, N. Matsumoto, *Inorg. Chem.* **1997**, *36*, 4329; c) P. M. Selvakumar, E. Suresh, P. S. Subramanian, *Polyhedron* **2009**, *28*, 245.
- [21] T. Honjo, M. Nakao, S. Sano, M. Shiro, K. Yamaguchi, Y. Sei, Y. Nagao, *Org. Lett.* **2007**, *9*, 509.
- [22] E. P. Kündig, A. E. Garcia, T. Lomberget, P. P. Garcia, P. Romanens, *Chem. Commun.* **2008**, 3519.

## SUPPORTING INFORMATION

Additional supporting information may be found online in the Supporting Information section at the end of the article.

**How to cite this article:** Chinnaraja E, Arunachalam R, Samanta J, Natarajan R, Subramanian PS. Desymmetrization of meso diols using enantiopure zinc (II) dimers: Synthesis and chiroptical properties. *Appl Organometal Chem.* 2019;e4827. <https://doi.org/10.1002/aoc.4827>